Chapter 2
MRI and MRCP

Il Kyoon Kim and Barton F. Lane

Abbreviations

CT	Computed tomography
DWI	Diffusion-weighted imaging
MIP	Maximal intensity projection
MRCP	Magnetic resonance cholangiopancreatography
MRI	Magnetic resonance imaging
(1.5 or 3) T	Tesla

Brief Introduction of MRI

MRI is acquired using the property of water molecules, specifically hydrogen protons, which behave as small magnets and align within the strong magnetic field, therefore requiring no radiation. Depending on pulse sequences, different soft tissue contrast can be achieved. For example, T1 sequences can highlight intrinsic blood, protein, melanin, and administered gadolinium-based contrast, while T2 can be used to identify edema, ascites, CSF, bile, and other fluids. Magnetic resonance cholangiopancreatography (MRCP) utilizes the T2 characteristics of fluid in bile to assess the biliary system [1]. More recently, diffusion-weighted imaging (DWI) has been incorporated into routine abdominal imaging. DWI captures the free motion of the water molecules and can magnify tissues that restrict that movement such as

I. K. Kim (✉) · B. F. Lane
University of Maryland Medical Center, Department of Diagnostic Radiology and Nuclear Medicine, Baltimore, MD, USA
e-mail: ilkyoon.kim@umm.edu; blane@som.umaryland.edu

N. Anand, P. Darwin (eds.), *Imaging Diagnostics in Pancreatic Cancer*, Clinical Gastroenterology, https://doi.org/10.1007/978-3-030-69940-6_2

tumor, ischemic tissue, abscess, and lymph nodes. For pancreatic adenocarcinoma, DWI is more sensitive than computed tomography (CT) for accentuating the tumor and also detecting lymph nodes and metastases, making it useful for staging [2].

Clinical MRI is available in various magnetic field strengths; however, the current standard of care for most imaging applications, and most commonly available scanners, has a field strength of 1.5 T (1.5 Tesla). 3 T strength MRI systems are becoming more widely available; however, while 3 T theoretically allows for higher signal to noise, in practice there is no appreciable imaging quality difference between 1.5 T and 3 T [3–6]. In fact, there are some limitations with 3 T MRI of the abdomen, which are beyond the scope of this chapter, and 1.5 T remains the standard of care for most abdominal MRI applications. As technology evolves, however, 3 T may ultimately replace 1.5 T systems.

Generally, patients fast for at least 4 hours to distend the gallbladder and to minimize artifacts related to motion from the stomach and regional bowel. As a complete evaluation protocol, many institutions use the following sequences: T2-weighted sequences; T1 in and opposed phases; T1-weighted sequences before and after intravenous administration of gadolinium-based contrast material at arterial, portal venous, and equilibrium phases (20–40 s, 45–65 s, and 3–5 min, respectively); 2D and 3D MRCP; and DWI [Table 2.1] [15, 16].

Additionally, while most images are routinely obtained in the axial plane, MRI allows for acquisition in any orientation, and coronal, sagittal, or other non-traditional planes of imaging can be acquired for many of the imaging sequences.

Patient Factors

While widely used, not all patients are suitable to undergo MRI. One major consideration is the presence of metallic foreign bodies such as cardiac or other electronic implants, embolization coils, endoscopic hemostatic clips, aneurysm clips, and

Table 2.1 Pancreatic mass MR protocol

Sequence	Plane	Utility
T2-weighted fast spin echo	Coronal +/− axial	Localization
T1-weighted in and opposed phase gradient echo	Axial	Fat-containing lesions
T2-weighted fat-suppressed fast spin echo	Axial	Cystic lesions
Diffusion-weighted imaging	Axial	Solid and cystic lesions; lymph nodes; metastases
Pre- and dynamic post-IV gadolinium 3D T1-weighted fat-suppressed gradient echo	Axial	Lesion characterization; vasculatures
T2-weighted MRCP	Coronal	Biliary ducts

Adapted with permission from the NCCN Guidelines® for Pancreatic Adenocarcinoma V.3.2019 [15]

shrapnel/bullet fragments. The most important concern with metallic objects is patient safety; ferromagnetic objects can be deflected by the magnetic field with potential for damage to adjacent tissues and organs. Magnetic fields can also induce electrical currents within wires or circular metallic objects leading to heating and potential thermal injury. However, many metallic implants are considered MRI compatible and do not necessarily preclude patients from undergoing imaging. By carefully assessing MRI compatibility of the device and risk, MRI can be safely performed [7]. All MRI facilities utilize extensive checklists to ensure that a patient scheduled for an exam is safe to undergo the procedure. The third issue with metallic objects is not related to safety but to image quality. Some metallic objects, although safe for imaging, can cause local alterations to the magnetic field and lead to significant image artifacts limiting diagnostic quality. For example, embolization coils in the gastroduodenal artery or endoscopic hemostatic clips in the duodenum may preclude evaluation of the adjacent pancreas due to associated susceptibility artifact [Fig. 2.1].

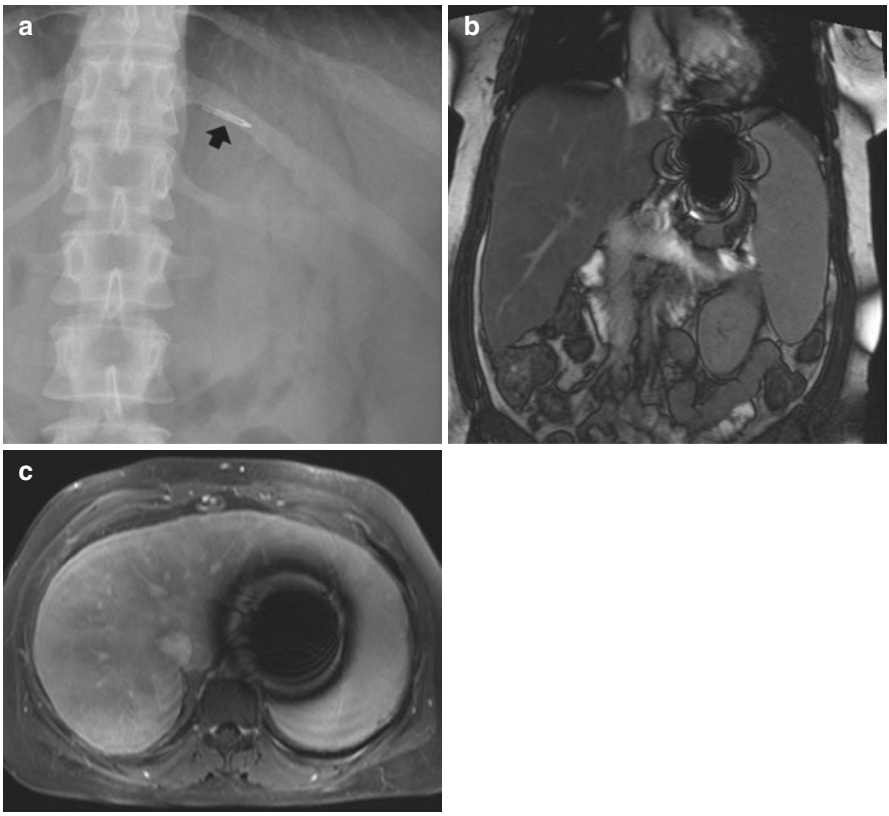

Fig. 2.1 (**a**) A metallic surgical clip in the left upper quadrant (black arrow) as noted in the abdominal radiograph can create (**b**, **c**) MRI susceptibility artifact and limit the evaluation of the surrounding structures

Obesity is a factor to consider, as MRI scanners typically have lower table weight limits and smaller bore size than CT scanners, and some patients may not be physically able to undergo MRI. However, newer MRI machines have larger bore sizes equivalent to CT (70 cm). So-called "open MRI" scanners can accommodate some of these patients, but usually at the expense of image quality given lower magnetic field strengths (typically 0.2–1.2 T). Even with a larger bore size, the MRI bore length is significantly greater than that of a CT scanner, frequently leading to patient anxiety and claustrophobia which may lead to early termination of the scan or outright refusal. Estimates are that 1–15% of patients are unable to complete an MRI scan secondary to claustrophobia [8, 9].

Other patient factors do not necessarily preclude patients from undergoing MRI but may adversely affect image quality leading to a suboptimal study. MRI of the abdomen requires a much longer scan time than CT, approximately 30–40 minutes for a complete study. Some of the imaging sequences require minutes and are obtained with free-breathing; others require 10–20 seconds and are obtained with breath-holds. Suboptimal breath-holding as well as irregular breathing can lead to artifacts degrading image quality; this is much less of an issue with modern CT scanners. Also, as MRI utilizes the characteristics of water molecules to create images, the presence of large fluid collections, ascites, and soft tissue edema/third spacing can deteriorate imaging quality, particularly MRCP [Fig. 2.2].

Probably the most commonly encountered patient condition regarding suitability for MRI is renal dysfunction. Gadolinium contrast agents are not nephrotoxic and do not impart a risk for impairing renal function even in patients with end-stage renal disease. However, since the FDA initially reported an association between nephrogenic systemic fibrosis (NSF) and gadolinium-based contrast agent administration, it has been found that patients were at increased risk with severe renal dysfunction (GFR <30) and specific types of contrast agents (termed group 1 agents).

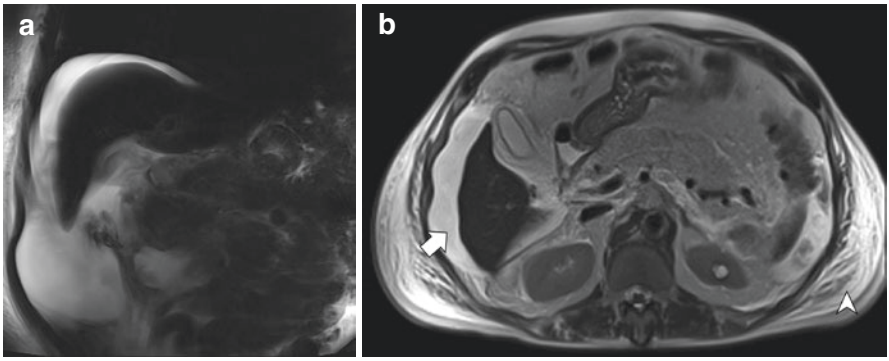

Fig. 2.2 (**a**) Biliary ducts on MRCP coronal images are not well visualized due to (**b**) artifacts from the ascites (white arrow) and anasarca (arrow head) as seen on the axial T2 sequence

With continued research and experience, however, it has been realized that there is very low or negligible risk of NSF development, regardless of renal function status, with what are termed group 2 agents. In conjunction with improved screening of patients for renal dysfunction and change in practice to using group 2 agents, the incidence of NSF has essentially been eliminated. The current American College of Radiology Contrast Manual recommends usage of group 2 gadolinium agents for renally impaired patients requiring contrast-enhanced MRI [10]. Many institutions and imaging centers have switched to using exclusively group 2 contrast agents, in which case screening for renal dysfunction may no longer be necessary. In short, even patients with renal dysfunction can safely undergo contrast-enhanced MRI with current screening standards and modern contrast agents.

Role of MRI

With MRI's higher sensitivity compared to CT in determining resectability of tumor (93% vs. 87%), vascular infiltration (80% vs. 50%), and liver involvement (90–100% vs. 70–76%), it is a useful tool in tumor staging [10–13]. As such, the American Society of Clinical Oncology (ASCO) recommends MRI as a part of the initial assessment after histopathologic confirmation of pancreatic adenocarcinoma diagnosis and before initiating therapy [14]. The National Comprehensive Cancer Network guidelines also suggest MRI as a problem-solving tool for initial workup and treatment response surveillance in addition to the multi-detector CT [15]. Especially for small, isoattenuating, or CT indeterminant masses, high soft tissue contrast of MRI is superb for diagnosis. MRCP is also a noninvasive way to evaluate for small mural nodules or differentiate stones from masses. With a combination of these characteristics, MRI and MRCP aid in early detection, staging, and surveillance of pancreatic cancer.

Imaging Characteristics of Pancreatic Cancer

Normal Versus Pancreatic Cancer

The normal pancreas typically has high signal on non-contrast-enhanced T1 fat-suppressed sequences. Following contrast administration, there is homogeneous intense enhancement during the early arterial phase which becomes isointense to the liver on later phases [Fig. 2.3]. Pancreatic adenocarcinoma generally appears hypointense compared to the surrounding parenchyma on T1 fat-suppressed images. It is also hypoenhancing and is best delineated during the late arterial

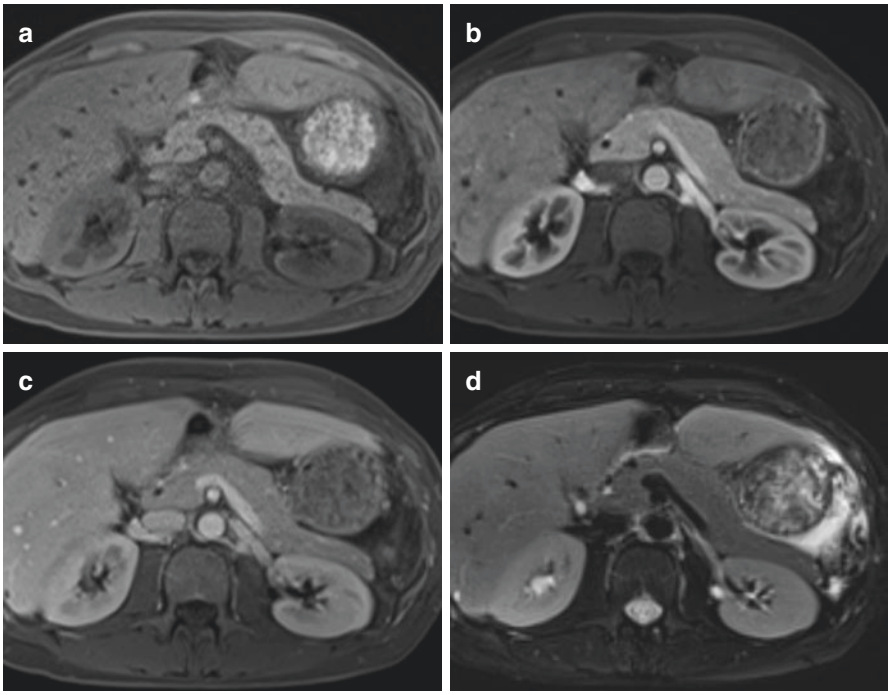

Fig. 2.3 Normal pancreas enhancement pattern. (**a**) In non-contrast T1 fat-suppressed sequence, the normal pancreas is brighter than the liver and spleen. (**b**) During the early arterial phase, the pancreas enhances homogeneously and (**c**) becomes isointense to the liver during delayed phases. (**d**) On equilibrium post-contrast sequence, the pancreas appears darker than the liver

phase as hypoenhancing tissue relative to the surrounding pancreatic parenchyma, with progressive enhancement on later post-contrast phases [Fig. 2.4] [16, 17]. These imaging characteristics may be due to fibrotic characteristic of pancreatic cancers [17, 18].

Secondary signs related to obstruction of the pancreatic duct, such as peripheral pancreatic ductal dilation and atrophy of the pancreatic tissue peripheral to the tumor, also aid in the detection of the tumor on MRI. Ductal dilation in particular is best visualized on MRCP, and a hallmark feature of pancreatic adenocarcinoma is dilation of both the common bile duct and the pancreatic duct, or "double duct sign" [Fig. 2.5]. Although not entirely specific to malignancy, it is commonly seen with pancreatic cancer [17].

Diffusion-weighted imaging has particular sensitivity for detecting pancreatic adenocarcinoma. Lesions that may not be detectable on contrast-enhanced CT, or subtle on other MRI sequences, can be readily demonstrated [Fig. 2.6].

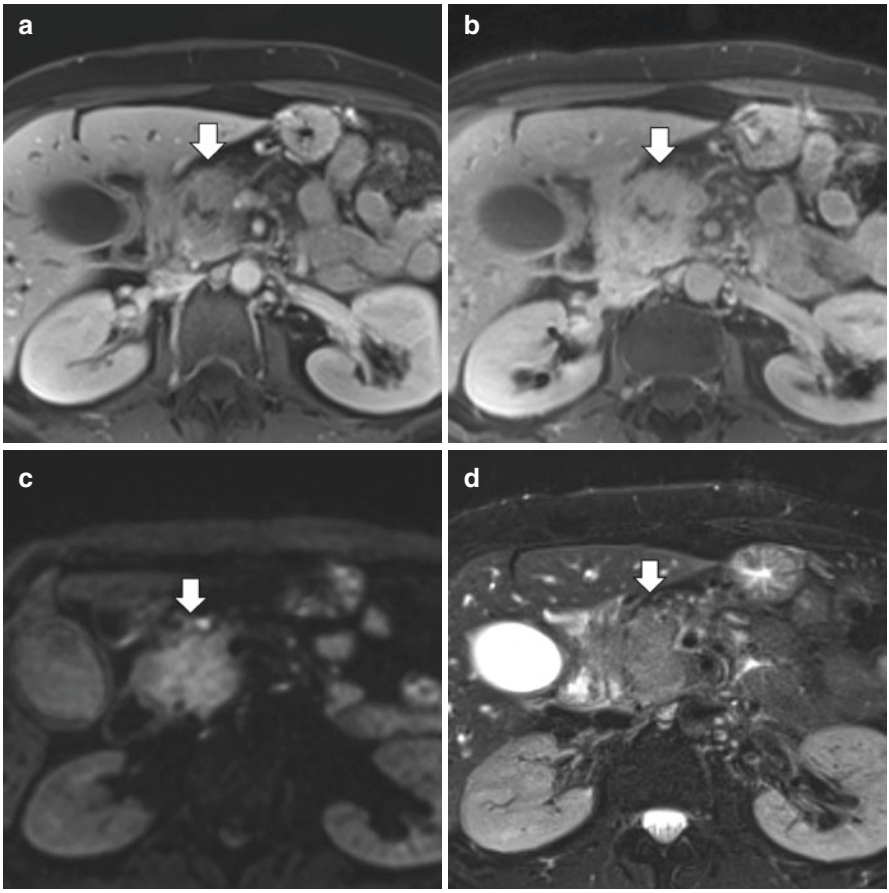

Fig. 2.4 Pancreatic adenocarcinoma (white arrow) at the head of the pancreas shows (**a**) hypoenhancement during the early arterial phase and (**b**) progressive enhancement on the delayed phase. (**c**) It also appears bright on DWI as it restricts diffusion. (**d**) On T2, the mass can be seen with intermediate signal and vague margins

Metastatic Disease

Liver

Identifying and characterizing liver lesions is critical in determining the resectability of pancreatic adenocarcinoma. Small lesions that may be indeterminate on CT imaging can be more definitively characterized with MRI. Relative to the surrounding liver parenchyma, metastases are minimally hypointense on T1-weighted sequences and isointense to moderately hyperintense on T2-weighted sequences. Contrast enhancement pattern varies, from peripheral ring enhancement to wedge-shaped

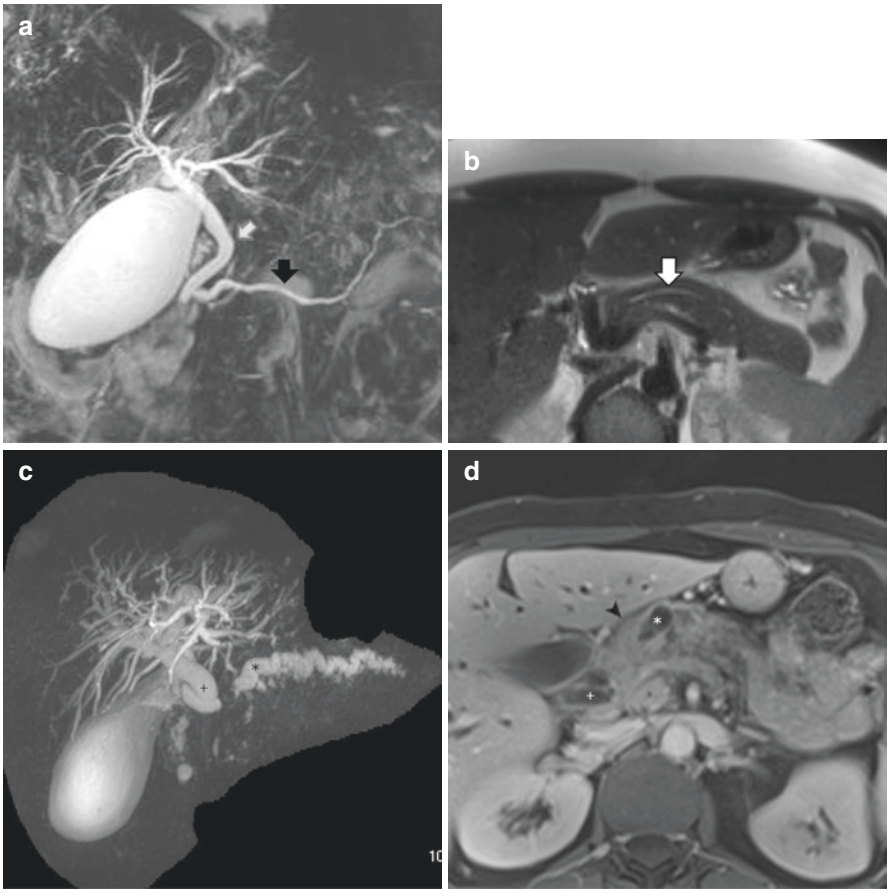

Fig. 2.5 (**a**) Normal MRCP maximal intensity projection (MIP) shows nondilated common bile duct (white arrow) and pancreatic duct (white arrow). (**b**) Corresponding T2 sequence shows a normal pancreatic duct (white arrow). In contrast, (**c**) "double duct sign" can be seen in the abnormal MRCP MIP with dilation of both the common bile duct (+) and the pancreatic duct (*) due to (**d**) the pancreatic head mass (black arrow head) in this T1 sequence in early arterial phase. Dilated common bile (+) and pancreatic ducts (*) are again seen adjacent to the mass

with differences in vascularity of the lesion [17]. DWI also can aid in detecting small metastases that can be overlooked in other sequences [Fig. 2.7].

Peritoneum and Lymph Nodes

Peritoneal involvement is common, however, in small volume, making detection difficult. MRI is found to be more sensitive than CT in detecting subcentimeter enhancing peritoneal implants [17, 19]. Peripancreatic and porta hepatis lymph

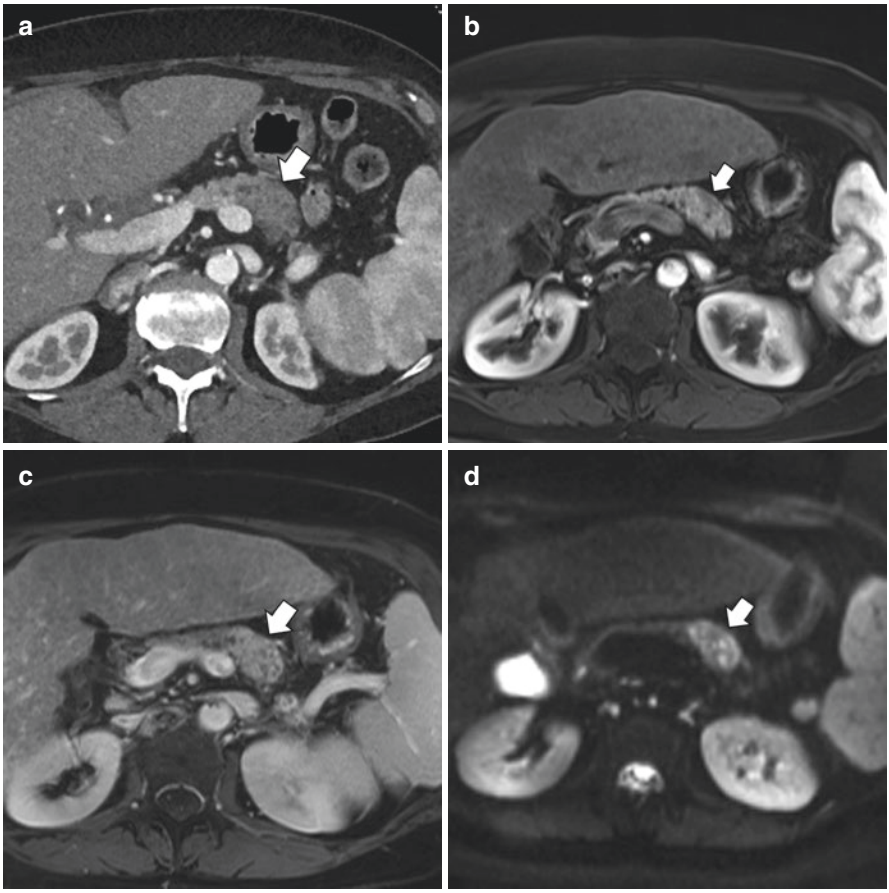

Fig. 2.6 (**a**) Subtle hypoenhancing pancreatic body lesion (white arrow) on CT also appears subtle on (**b**) the arterial phase of T1 sequence MRI as a hypoenhancing mass with (**c**) progressive enhancement on the delayed phase. (**d**) On DWI, however, the mass restricts diffusion and is readily seen

node involvement is also common and can be seen as enlarged (> 1 cm in short axis) and bright (diffusion restricting) lesions on DWI sequence [Fig. 2.8]. MRI is more sensitive than CT for the detection of lymph nodes, although still limited in characterizing benign versus malignant nodes as size remains the primary factor.

Vascular

Vascular invasion by tumor, especially the celiac artery, superior mesenteric artery, superior mesenteric vein, and portal vein, is an important factor in determining tumor resectability. T1 fat-suppressed images and gadolinium

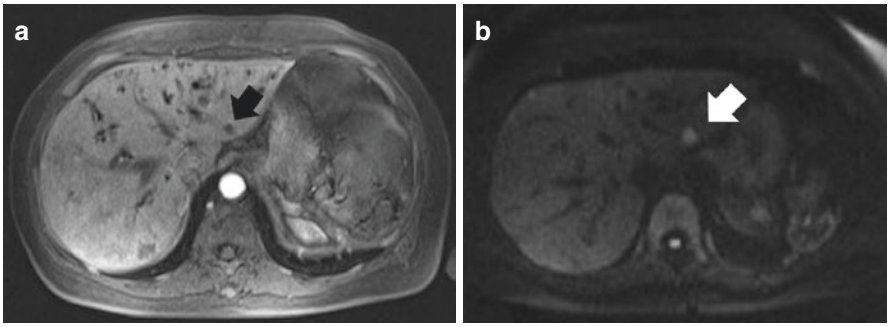

Fig. 2.7 (**a**) Small hypoenhancing liver metastatic lesion (black arrow) on arterial phase of T1 sequence is readily visible on (**b**) the DWI sequence (white arrow)

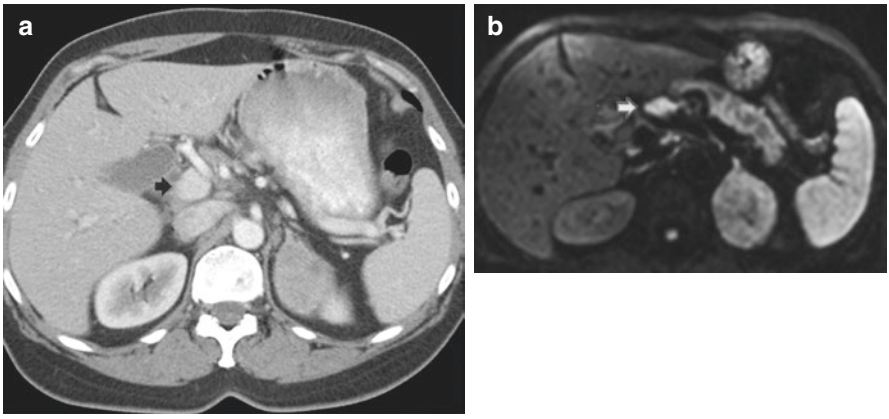

Fig. 2.8 (**a**) A lymph node (black arrow) by the porta hepatis is noted in a contrast-enhanced CT in arterial phase. (**b**) The same lymph node (white arrow) is seen restricting diffusion and bright on MR DWI sequence

contrast-enhanced images can aid in differentiating abutment versus encasement of vasculature [Fig. 2.9] [17].

Future Trends in Pancreatic Adenocarcinoma Imaging

Positron emission tomography (PET) combined with CT is a useful tool in diagnosis, initial staging, and treatment response for pancreatic adenocarcinoma. With the recent advent of concurrent PET/MRI scanners, many clinical studies are underway for assessing different cancer imaging [20–25]. Currently available concurrent scanners combine PET detectors with co-located 3 T MRI detectors for better co-registration of images. Generally, protocols include whole-body MRI survey

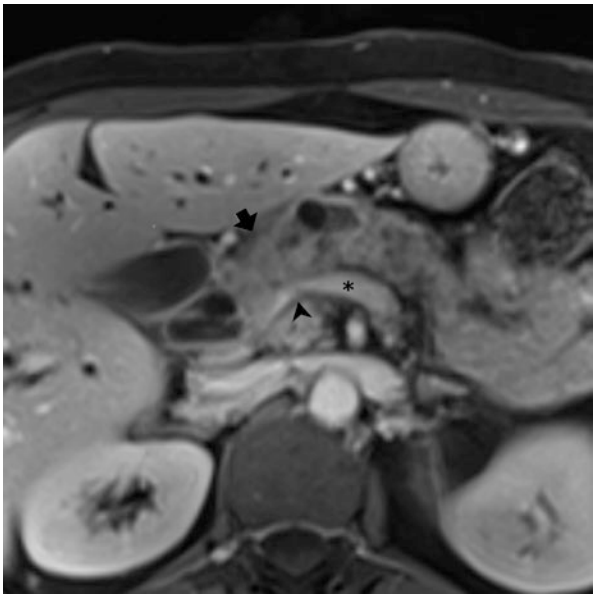

Fig. 2.9 Venous phase of the T1 sequence clearly delineates the splenic vein (*) with gradual narrowing (arrow head) due to encasement from the surrounding pancreatic head mass (arrow)

component with organ-specific focused MRI sequences for better characterization of liver, peritoneal, lymph node, or vascular involvement [20]. With the high sensitivity of PET imaging and superior soft tissue contrast resolution of MRI, combined PET/MRI has the potential to increase accuracy in early detection, staging, and recurrence.

References

1. Grover VP, Tognarelli JM, Crossey MM, Cox IJ, Taylor-Robinson SD, McPhail MJ. Magnetic resonance imaging: principles and techniques: lessons for clinicians. J Clin Exp Hepatol. 2015;5(3):246–55.
2. De Robertis R, Tinazzi Martini P, Demozzi E, Dal Corso F, Bassi C, Pederzoli P, et al. Diffusion-weighted imaging of pancreatic cancer. World J Radiol. 2015;7(10):319–28.
3. Scialpi M, Reginelli A, D'Andrea A, Gravante S, Falcone G, Baccari P, et al. Pancreatic tumors imaging: an update. Int J Surg. 2016;28(Suppl 1):S142–55.
4. Kim SY, Byun JH, Lee SS, Park SH, Jang YJ, Lee MG. Biliary tract depiction in living potential liver donors: intraindividual comparison of MR cholangiography at 3.0 and 1.5 T. Radiology. 2010;254(2):469–78.
5. Schmidt GP, Wintersperger B, Graser A, Baur-Melnyk A, Reiser MF, Schoenberg SO. High-resolution whole-body magnetic resonance imaging applications at 1.5 and 3 Tesla: a comparative study. Investig Radiol. 2007;42(6):449–59.
6. Goncalves Neto JA, Altun E, Elazzazi M, Vaidean GD, Chaney M, Semelka RC. Enhancement of abdominal organs on hepatic arterial phase: quantitative comparison between 1.5- and 3.0-T magnetic resonance imaging. Magn Reson Imaging. 2010;28(1):47–55.
7. Kanal E, Barkovich AJ, Bell C, Borgstede JP, Bradley WG, Froelich JW, et al. ACR guidance document on MR safe practices: 2013. J Magn Reson Imaging. 2013;37(3):501–30.

8. Dewey M, Schink T, Dewey CF. Claustrophobia during magnetic resonance imaging: cohort study in over 55,000 patients. J Magn Reson Imaging. 2007;26(5):1322–7.
9. Munn Z, Jordan Z. Interventions to reduce anxiety, distress and the need for sedation in adult patients undergoing magnetic resonance imaging: a systematic review. Int J Evid Based Healthc. 2013;11(4):265–74.
10. Qayyum A, Tamm EP, Kamel IR, Allen PJ, Arif-Tiwari H, Chernyak V, et al. ACR appropriateness criteria. J Am Coll Radiol. 2017;14(11S):S560–S9.
11. Koelblinger C, Ba-Ssalamah A, Goetzinger P, Puchner S, Weber M, Sahora K, et al. Gadobenate dimeglumine-enhanced 3.0-T MR imaging versus multiphasic 64-detector row CT: prospective evaluation in patients suspected of having pancreatic cancer. Radiology. 2011;259(3):757–66.
12. Zhang Y, Huang J, Chen M, Jiao LR. Preoperative vascular evaluation with computed tomography and magnetic resonance imaging for pancreatic cancer: a meta-analysis. Pancreatology. 2012;12(3):227–33.
13. Motosugi U, Ichikawa T, Morisaka H, Sou H, Muhi A, Kimura K, et al. Detection of pancreatic carcinoma and liver metastases with gadoxetic acid-enhanced MR imaging: comparison with contrast-enhanced multi-detector row CT. Radiology. 2011;260(2):446–53.
14. Khorana AA, McKernin SE, Katz MHG. Potentially curable pancreatic adenocarcinoma: ASCO clinical practice guideline update summary. J Oncol Pract. 2019;15(8):454–7.
15. National Comprehensive Cancer Network. Pancreatic adenocarcinoma (Version 3.2019). Available from: https://www.nccn.org/professionals/physician_gls/pdf/pancreatic.pdf.
16. Lee ES, Lee JM. Imaging diagnosis of pancreatic cancer: a state-of-the-art review. World J Gastroenterol. 2014;20(24):7864–77.
17. Miller FH, Rini NJ, Keppke AL. MRI of adenocarcinoma of the pancreas. AJR Am J Roentgenol. 2006;187(4):W365–74.
18. Manikkavasakar S, AlObaidy M, Busireddy KK, Ramalho M, Nilmini V, Alagiyawanna M, et al. Magnetic resonance imaging of pancreatitis: an update. World J Gastroenterol. 2014;20(40):14760–77.
19. Krishnamurthy S, Balasubramaniam R. Role of imaging in peritoneal surface malignancies. Indian J Surg Oncol. 2016;7(4):441–52.
20. Yeh R, Dercle L, Garg I, Wang ZJ, Hough DM, Goenka AH. The role of 18F-FDG PET/CT and PET/MRI in pancreatic ductal adenocarcinoma. Abdom Radiol (NY). 2018;43(2):415–34.
21. Salamon N, Kung J, Shaw SJ, Koo J, Koh S, Wu JY, et al. FDG-PET/MRI coregistration improves detection of cortical dysplasia in patients with epilepsy. Neurology. 2008;71(20):1594–601.
22. Romeo V, Iorio B, Mesolella M, Ugga L, Verde F, Nicolai E, et al. Simultaneous PET/MRI in assessing the response to chemo/radiotherapy in head and neck carcinoma: initial experience. Med Oncol. 2018;35(7):112.
23. Heusch P, Buchbender C, Köhler J, Nensa F, Beiderwellen K, Kühl H, et al. Correlation of the apparent diffusion coefficient (ADC) with the standardized uptake value (SUV) in hybrid 18F-FDG PET/MRI in non-small cell lung cancer (NSCLC) lesions: initial results. Rofo. 2013;185(11):1056–62.
24. Kang B, Lee JM, Song YS, Woo S, Hur BY, Jeon JH, et al. Added value of integrated whole-body PET/MRI for evaluation of colorectal cancer: comparison with contrast-enhanced MDCT. AJR Am J Roentgenol. 2016;206(1):W10–20.
25. Barbaro B, Vitale R, Leccisotti L, Vecchio FM, Santoro L, Valentini V, et al. Restaging locally advanced rectal cancer with MR imaging after chemoradiation therapy. Radiographics. 2010;30(3):699–716.